Crystallization and Morphology of Poly(ethylene oxide)-*p*-Nitrophenol Molecular Complex Crystallized from the Melt

P. Damman and J. J. Point*

Laboratoire de Chimie Physique et Thermodynamique, Université de Mons Hainaut, 20, place du Parc, B-7000 Mons, Belgium

Received October 6, 1992; Revised Manuscript Received November 23, 1992

ABSTRACT: We report here a study on the crystallization of a new crystalline complex made from poly(ethylene oxide) (PEO) and *p*-nitrophenol (pnp). The crystal structure of this complex was previously determined by X-ray diffraction and polarized FTIR. When the molecular weight of the polymeric component is either 6000 or 35 000, melt-grown crystals exist as non-integral-folded (NIF) lamellae and not as the integral-folded (IF) species generally observed for pure oligomeric PEO. Consequently, it may be presumed that the mode of growth of such a complex is similar to that of a high molecular weight polymer. We have measured the linear spherulitic growth rates of the complex in the crystallization temperature range of 25-70 °C. The log G versus T_c curves are surprisingly similar for both molecular weights, which present three branches with two intersection points at T_c = 58 and 65 °C (the same temperature for both M_w). From X-ray diffraction patterns and polarized FTIR spectra of the PEO-pnp spherulites, we observed that, for crystallization temperatures below 58 °C and above 65 °C, the growth face is (100) but, in between these two temperatures, the leading facet corresponds to a (010) crystallographic face. This is an additional example where the breaks in the curve giving the thermal dependence of the growth rate are not signatures of regime transitions.

Introduction

The complex of poly(ethylene oxide) (PEO) made from inorganic molecules such as $HgCl_2$[1] or NaI[2] and from organic molecules such as *p*-dihalogenobenzene[3] or resorcinol[4,5] are widely known. This paper deals with the PEO-*p*-nitrophenol (pnp) complex recently prepared in our laboratory. The crystal structure of the α form of this complex was previously determined from X-ray diffraction[6] and from FTIR studies.[7] The unit cell is triclinic and contains 6 PEO monomeric units and 4 pnp molecules stacked along the c crystallographic axis. In fact, the complex is made of parallel layers of PEO and pnp molecules stacked along the a^* reciprocal axis (Figure 1). In this paper, we consider how observed breaks in curves giving the thermal dependence of the linear crystal growth rate of spherulites of the PEO-pnp complex might be explained using different assumptions.

(a) Currently observed in polymer crystallization, these breaks are usually interpretated as I-II or II-III regime transitions.[8,9] More particularly, breaks observed in curves giving the thermal dependence of the growth rate of spherulites of pure PEO were interpreted by Allen and Mandelkern[10] as being due to different regime transitions. However, a recent alternative has been given by us in collaboration.[11] A critical review of the interpretation of breaks, considered as regime transitions in different polymer systems studied in the literature, was done by one of us in collaboration with J. J. Janimak.[12]

(b) Skoulios et al.,[13] Kovacs et al.,[14] and Cheng et al.[15] have reported that lamellar crystals of low molecular weight (M_w) PEO were integral-folded (IF). Kovacs et al. have related the breaks observed in the log(G) versus T_c curves of spherulites and that of single crystals of low M_w PEO to a change in conformation of the macromolecules.[16] Successively, and in partially overlapping temperature ranges, the PEO molecules in the lamellae are folded with integral numbers of folds (n) or extended (n = 0). Each range of crystallization temperature corresponds to a well-defined value of n and is limited by a transition temperature which corresponds to the breaks in the growth rate versus T_c curve. We note however that non-integral-folded (NIF) crystals were observed by SAXS, at the onset of crystallization, by Cheng.[15] These NIF crystals are relatively unstable and quickly transform into IF crystals by thickening or thinning processes.

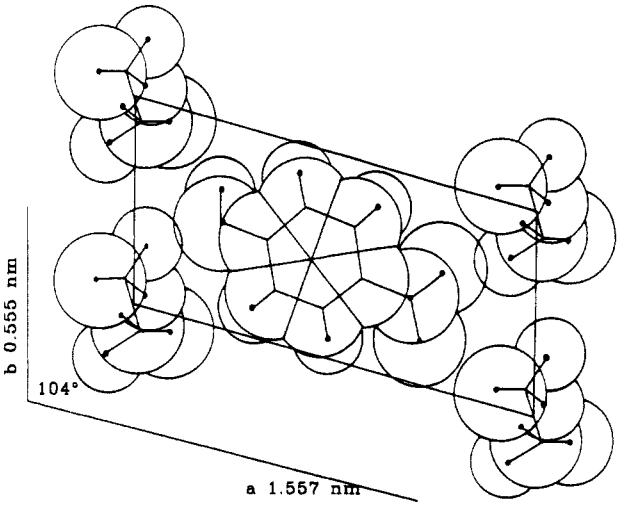

Figure 1. Crystal structure of the PEO-pnp molecular complex.

(c) Finally, Hirai et al.[17] have reported the observation of two different leading facets in spherulites of pure PEO, depending upon crystallization conditions. We have also reported that one of the breaks observed in the log G versus T_c curve for a medium M_w PEO corresponds exactly to a change of crystal orientation with respect to the radius of the spherulite. In fact, for T_c below or above 49.7 °C, we have observed (010) or (120) leading facets, respectively. Different crystal orientations, namely, (010) and (120), were found by Balta-Calleja et al.[18] (also for spherulites). However, their observations were not related to growth rate measurements.

In order to confirm if one or more of these explanations apply to the PEO-pnp complex, we have studied spherulites of this material by differential scanning calorimetry, wide-angle and small-angle X-ray diffraction, Fourier transform infrared spectroscopy, and optical microscopy.

0024-9297/93/2226-1722$04.00/0

Experimental Section

Preparation of the Samples. The samples were made from PEO (M_w = 6000 and 35 000 from Hoechst) and pnp by melting stoichiometric mixtures of the two components. The stoichiometry was previously determined by calorimetry and was found to correspond to 6 pnp molecules for 4 PEO monomeric units.

DSC Measurements. The samples were measured with a Perkin-Elmer DSC4. The DSC was calibrated using indium and benzoic acid as standards. Measurements were performed at a heating rate of 10 °C/min in sealed aluminum cells containing 3–6 mg of the PEO–pnp complex.

Small-Angle and Wide-Angle X-ray Scattering. SAXS and WAXS measurements were performed on a Rigaku Denki RU-200D Rotaflex generator. The radiation used was Cu Kα of wavelength 0.154 18 nm. X-ray diffraction patterns of spherulites of the PEO–pnp complex were recorded with a modified point focused Kissieg camera with flat plates. The sample to film distance was 36 mm and calibrated with silver. SAXS investigations were carried out with a modification point focused Kissieg camera with a sample to film distance of 400 nm.

Polarized Optical Microscopy. Polarized optical microscopy observations of the PEO–pnp complex were carried out on a Leitz Wetzlar Ortholux microscope, in conjunction with a Mettler FP52 hot stage. The hot stage was calibrated with standard melting substances in the used temperature range. Sample films of the complex approximately 10 μm thick were prepared between coverslip and microscope slide. The growth rates of the spherulites and/or hedrites of the complex were measured in regular time intervals prior to impingement effects. This procedure was repeated several times at each crystallization temperature with a standard deviation lower than ±5%.

FTIR Spectroscopy. IR spectra were taken with a Bruker IFS 113V Fourier transform infrared spectrometer. The polarized spectra of the spherulites were recorded with an aluminum wire grid polarizer. Thirty-two interferograms were coadded with a resolution of 1 cm^{-1}.

Results

Crystallization Kinetics of Spherulites of the Complex. As shown by the SAXS measurements, the PEO–pnp complex crystallizes from the melt as lamellae. It is inferred that the mode of growth of the spherulites is dictated by the polymeric component of the molecular complex. In fact, we observe a linear growth of spherulite size with time for different crystallization temperatures (T_c) as previously reported for the pure polymer.[19] We also observed that when spherulites impinge, a reduction of the growth rate occurs, which may be attributed to the accumulation of low molecular weight PEO between the spherulites or to small differences in composition with respect to the stoichiometry. The thermal dependences of the logarithm of growth rates are shown in Figures 2 and 3 for both of the complexes studied, PEO(M_w = 6000)–pnp and PEO(M_w) = 35 000)–pnp. From these figures, we can clearly see two breaks which occur at T_c = 58 and 65 °C. We note here that these transition temperatures are surprisingly the same for both molecular weights.

Differential Scanning Calorimetry and Small-Angle X-ray Scattering. The melting temperature of PEO(M_w = 6000)–pnp versus crystallization temperature is given in Figure 4. The melting temperature varies continuously with T_c, and only a single endotherm is observed. Multiple endotherms, which are generally observed for oligomeric PEO, are attributed to the different IF crystals. The discontinuous variation of the melting temperature was also related to the existence of IF crystals.[14-15]

The measurement of the lamellar thickness of the PEO-(M_w = 6000)–pnp complex crystallized at different T_c confirms our calorimetric observations. Figure 5 shows that the fold lengths of the PEO–pnp crystals reside in the vicinity of two and three times folded. We note however that the SAXS patterns never exhibit an IF lamellar thickness.

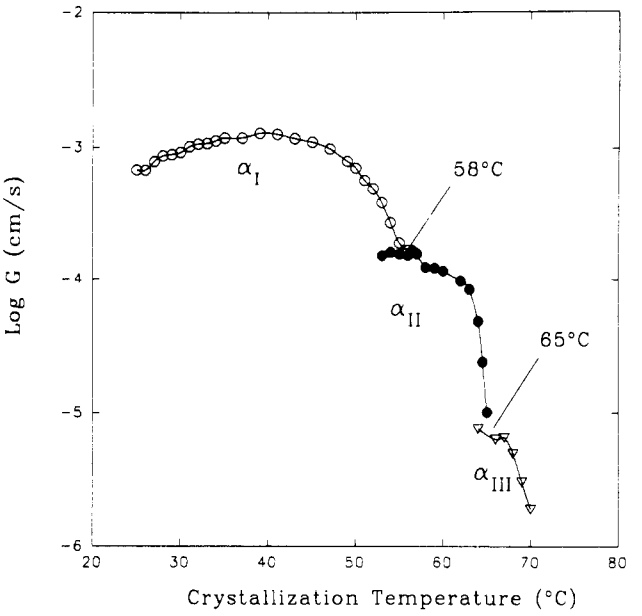

Figure 2. Thermal dependence of the linear growth rate of PEO-(M_w=6000)–pnp sperulites.

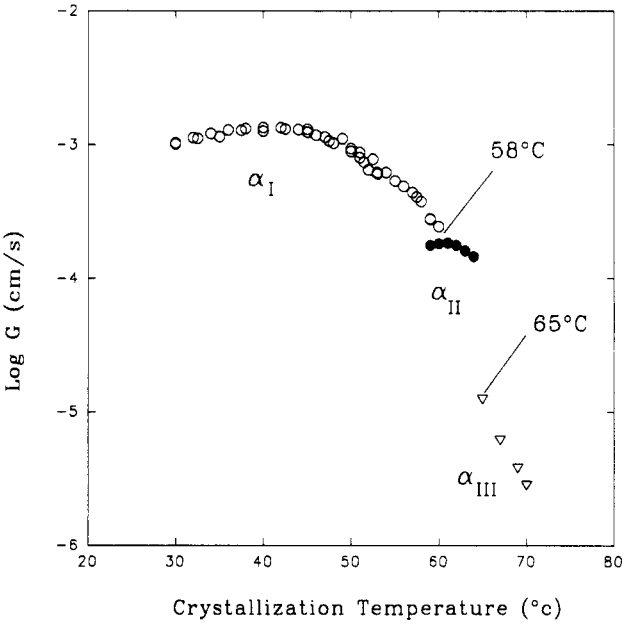

Figure 3. Thermal dependence of the linear growth rate of PEO-(M_w=35 000)–pnp spherulites.

Optical Microscopy. A selection of optical micrographs of spherulites between crossed polars are shown in Figure 6 at different crystallization temperatures. We have termed α_I, α_{II}, and α_{III} as the spherulites which crystallize in the three different domains delimited by the two breaks. The α_I type crystallized at 30 °C show a fine fibrous texture and a Maltese cross extinction pattern. At a crystallization temperature of 50 °C, the α_I sperulites begin to appear more coarse and the Maltese cross becomes less defined. However, we always observe a radial mode of growth. At 57 °C, the fibers become more thick and grow more or less independently. This type of growth leads to irregular-shaped spherulites. At a T_c of 58 °C, we observe a change in the morphology of the spherulites. This temperature range corresponds to spherulites grown in the α_{II} domain. These spherulites do not show a fibrous texture or a well-defined exctinction pattern. This morphology persists

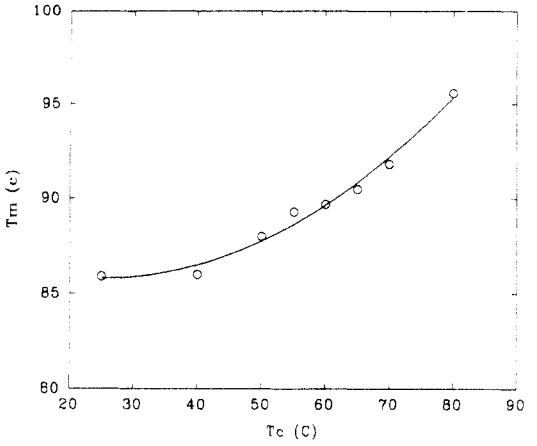

Figure 4. Melting temperatures of the PEO(M_w=6000)–pnp complex versus T_c.

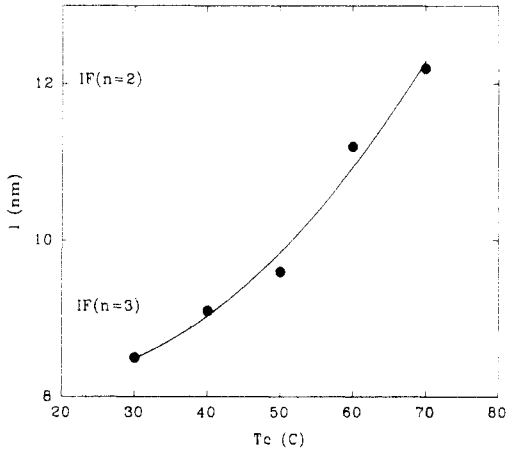

Figure 5. Thermal dependence of the lamellar thickness of PEO-(M_w=6000)–pnp.

until 65 °C where we observe a second sudden change, marked by the onset of the α_{III} spherulites. During the initial stages of crystallization, we observe hedrites similar to those reported by Geil for pure PEO.[20] The morphology of these crystals changes with increasing size and finally leads to a more ramified structure similar to that of a spherulite (with a cylindrical symmetry as revealed by its WAXS pattern). The growth rate measurements were done when cylindrical symmetry is achieved.

Wide-Angle X-ray Diffraction. X-ray diffraction patterns for the two complexes PEO(M_w = 6000)–pnp and PEO(M_w = 35 000)–pnp crystallized at 25, 30, 40, 50, 60, and 70 °C are shown in Figure 7. From the indexations of these diffraction diagrams which are based on a triclinic unit cell previously determined,[6] a = 1.172 nm, b = 0.555 nm, c = 1.557 nm, α = 90.7°, β = 87.1°, and γ = 104.0°, we note the following:

(a) The α_I and α_{III} spherulites, which are observed at low and high T_c, crystallize with a (100) growth face. The a^* reciprocal axis is along the radius of the spherulite.

(b) The α_{II} spherulite, which is observed at intermediate T_c, crystallizes with a (010) growth face. The b^* reciprocal axis is along the radius of the spherulite.

We note that, in Figure 7c, the equatorial (h00) reflections appear very weak by comparison with parts a, b, and d of Figure 7, in which the (h00) reflections are polar.

Polarized FTIR. From the crystal structure of the complex (Figure 1) and the dichroism observed for the pnp and PEO IR vibrations, the molecular orientation with respect to the radius of the spherulite was determined. In fact, this molecular orientation leads to an identification of the crystallographic leading facet of the spherulites. Figures 8–10 show polarized IR spectra of the α_I, α_{II}, and α_{III} spherulites. The dichroic behaviors of the observed IR bands are summarized in Tables I and II. From a normal-mode analysis of the PEO chains in the complex,[7] we have determined the conformation of the macromolecules and the direction of the transition moment of the PEO vibrations with respect to the unit cell. These directions are summarized as follows: the 455-, 1032-, and 1135-cm^{-1} vibrations are polarized along the a^* reciprocal parameter, and the 872-cm^{-1} vibration is polarized along the b crystallographic parameter. These assignments were confirmed by pleochroic measurements on double-oriented samples of the PEO–pnp complex prepared by stretching or rolling.[21] From Table II, it can be seen that the α_I and α_{III} spherulites have the 455-, 1032-, and 1135-cm^{-1} vibrations polarized parallel to the radius and the 871- and 947-cm^{-1} vibrations polarized perpendicular to the growth direction. These observations imply that the crystallographic growth face is (100) for the α_I and α_{III} spherulites as previously determined by X-ray diffraction. For α_{II}, the observed 871-cm^{-1} vibration is polarized parallel to the radius of the spherulite and the 455-, 947-, 1032-, and 1135-cm^{-1} vibrations are polarized perpendicular to the growth direction. This dichroic behavior is in agreement with the (010) crystallographic growth face proposed for the α_{II} spherulite. From Table I, it is observed that the dichroism of the pnp vibrations agrees with our proposal. The a1 benzenic vibrations are polarized parallel for the α_I and α_{III} spherulites; however, for the α_{II} species, only the b1 vibrations are polarized parallel to the growth direction. The FTIR spectra also give information about the interactions between host and guest molecules. Figure 11 shows the IR spectra of pure pnp and the PEO–pnp complex. The shift observed for the OH stretching vibration reveals that hydrogen bonds exist between the oxygen ethers of PEO and the pnp molecules themselves.

Discussion

Three explanations proposed to account for the origin of the observed breaks in the curves giving the thermal dependence of the linear growth rate of spherulites of the PEO–pnp complex will be discussed on the basis of experimental findings.

Regime Transitions. The log G versus T_c curves given in Figures 2 and 3 cannot be interpreted as signatures of regime I–II and II–III transitions. Such an interpretation would imply that $K_{gIII} > K_{gII} > K_{gI}$, and this inequality is clearly meaningless. Moreover, as seen in Figures 2 and 3, the experimental points lie on intersecting curves and not on a single curve with break points as would be the case for real regime transitions. The regime theory assumes that, at each T_c, the crystallization process proceeds in a unique way. At low supercooling, the kinetic length (given by $(2g/i)^{1/2}$) is so large that only one nucleus is initiated onto the growth face. At high supercooling, several nuclei are initiated simultaneously onto the growth face, and the kinetic length decreases accordingly. Finally, the kinetic length becomes so small that the crystallization proceeds by a rough surface growth mechanism. Hence, regimes I–III correspond to three different branches of one curve (log(G/β) versus $1/T\Delta T$) and to a single growth face. However, the regimes never correspond to three curves which may overlap. A change of regime of crystallization does not explain the observed breaks in the log G versus T_c curves for the PEO–pnp complex.

Mode of Folding. Our calorimetric and SAXS observations show that the PEO–pnp complex crystallizes only

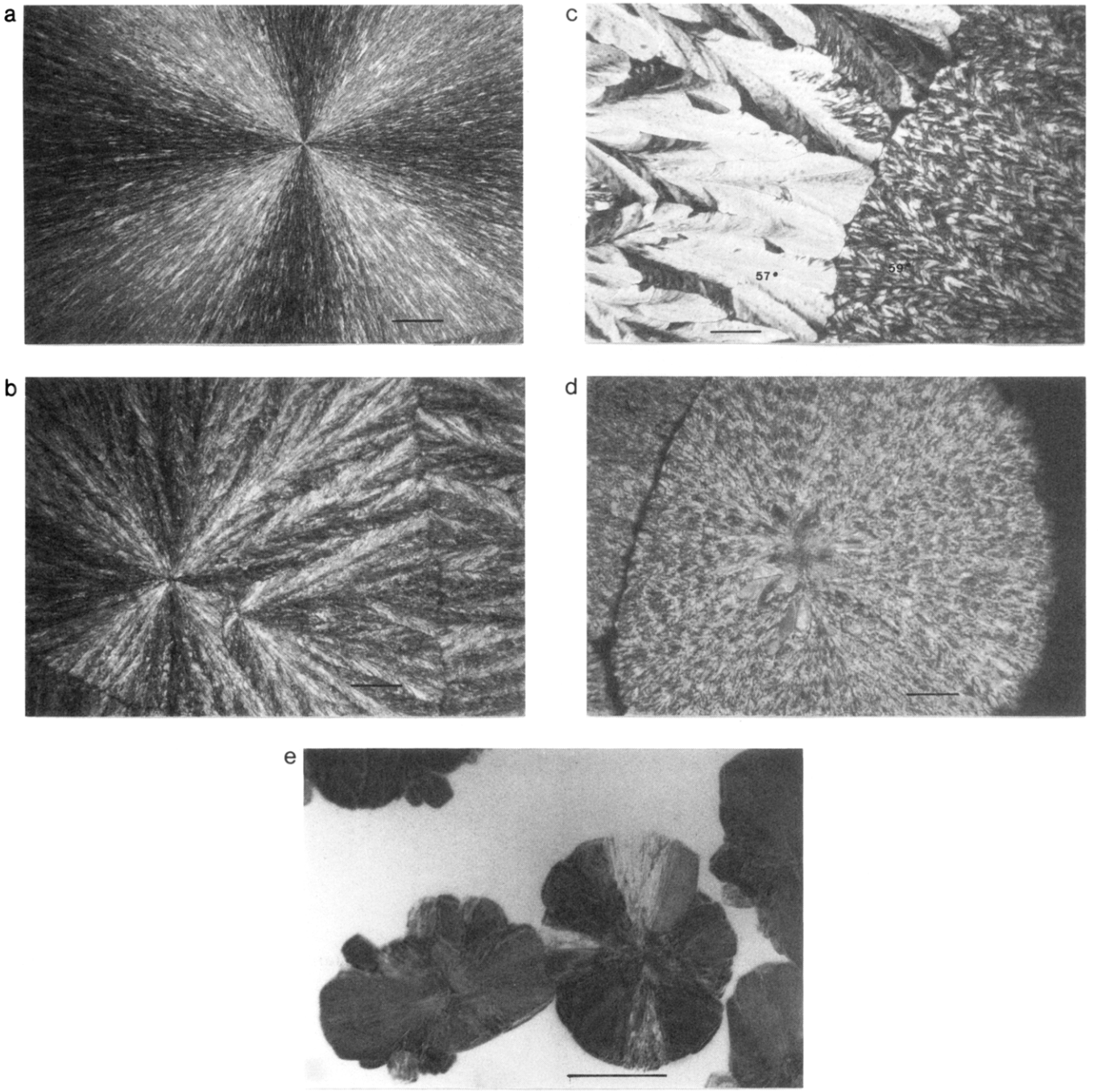

Figure 6. Selection of optical micrographs of PEO–pnp spherulites crystallized at different T_c: (a) 30, (b) 50, (c) 57–59, (d) 61, and (e) 70 °C. The scale bar corresponds to 100 μm.

as non-integral-folded lamellae. No transition (abrupt change) is observed in the melting temperature and lamellar thickness versus T_c curves. The correlation between the surface free energy, σ_e, with respect to the thickness of the lamellae l, appears to be not as straightforward as usually thought. A change in the mode of folding cannot be related to the breaks observed. The existence of IF crystals of PEO is generally explained on the basis of two assumptions, based on studies of differently end-capped PEO macromolecules.

Shimada et al.[22] have reported the observation of stable NIF crystals of PEO (M_w = 15 000, 7400, 2330) crystallized from solution and phenyl-end-capped PEO (M_w = 7090) crystallized from the melt. Thierry et al.[23] have also reported that phenyl-end-capped (M_w = 13 400) and octadecaoxy-ended (M_n = 11 400) PEO crystallize as NIF crystals. In both these studies, the lamellar thickness shows a continuous variation with T_c. The works of Shimada and Thierry seem to indicate the importance of hydrogen bonds in the formation of IF crystals. Moreover, Buckley and Kovacs explained the stability of IF crystals by the formation of hydrogen bonds between lamellae.[14]

By contradistinction, Fraser et al.[24] and more recently Cheng et al.[25] have reported that alkoxy-end-capped PEO with a M_w of 3000 exhibits IF crystal habits. Both these groups concluded that the hydrogen bonds do not influence the formation of IF crystals. We also note that the observation of IF lamellae of long paraffins has been found by Ungar et al.[26]

In our system, the PEO and pnp molecules do hydrogen bond as revealed by the FTIR study (Figure 11). We cannot expect that the formation of hydrogen bonds between OH pertaining to the same or different PEO molecules instead of the formation of hydrogen bonds between PEO and pnp molecules may modify significantly

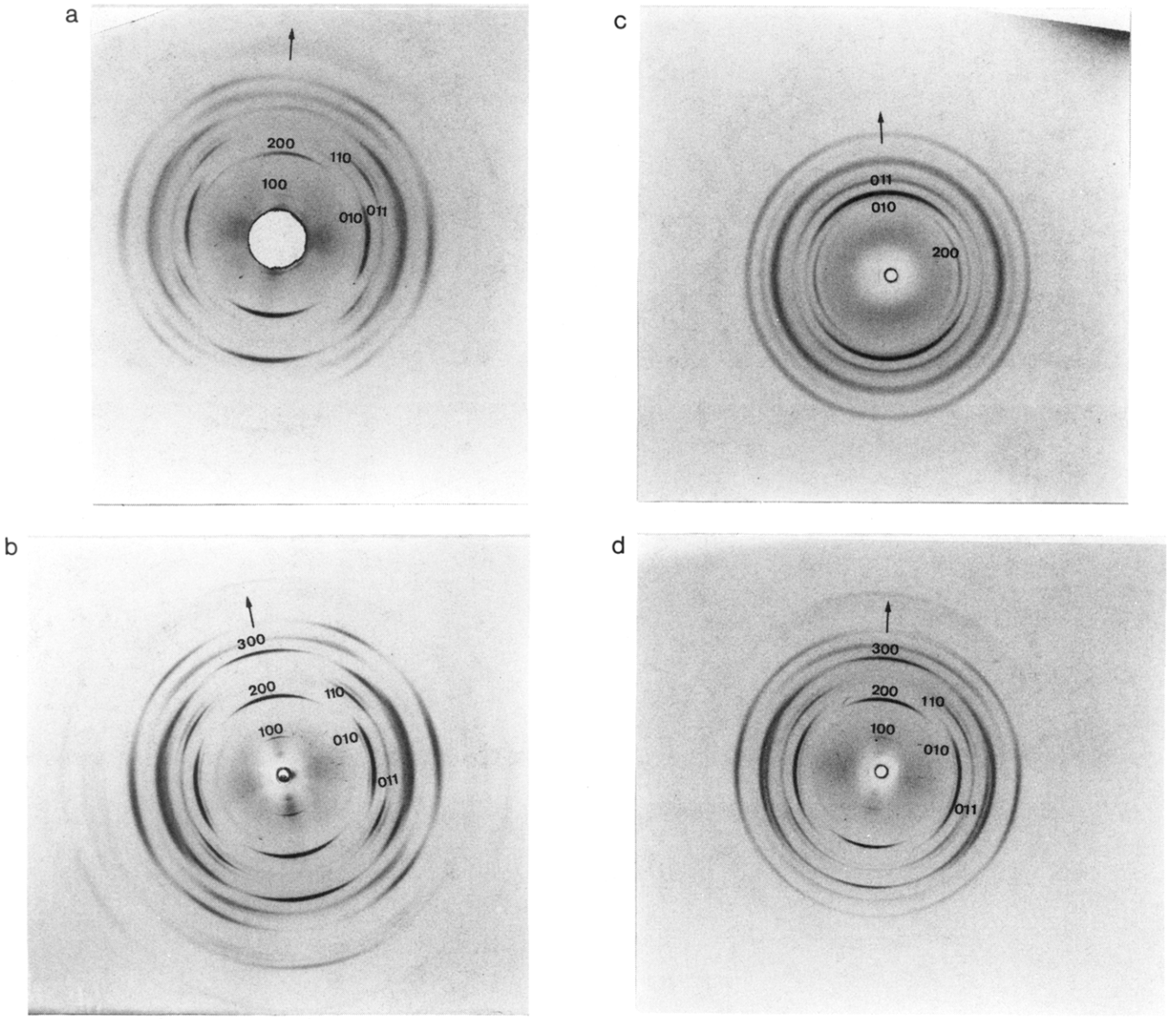

Figure 7. WAXS patterns of PEO(M_w=6000(–pnp spherulites crystallized at different T_c: (a) 30, (b) 50, (c) 60, and (d) 70 °C. The arrows indicate that fiber axes of the sperulites.

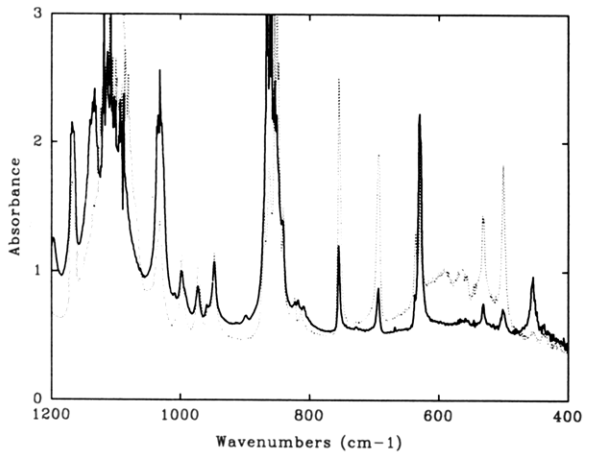

Figure 8. Polarized IR spectra of PEO(M_w=35 000)–pnp spherulites crystallized at 50 °C. The solid or broken lines correspond to an electric vector parallel or perpendicular to the radius of the spherulite, respectively.

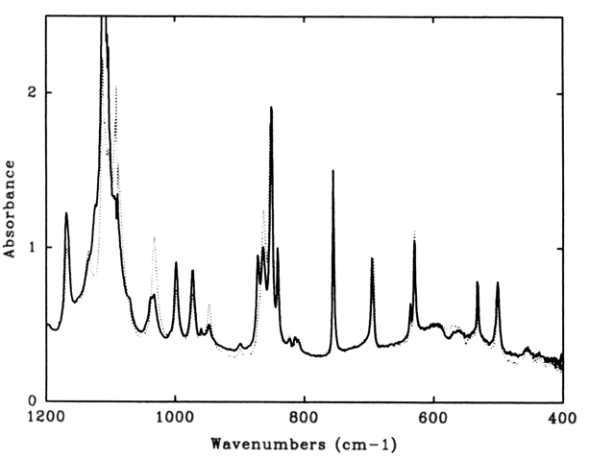

Figure 9. Polarized IR spectra of PEO(M_w=3500)–pnp spherulites crystallized at 61 °C. The solid or broken lines correspond to an electric vector parallel or perpendicular to the radius of the spherulite, respectively.

the value of the free energy and may induce preferentially the formation of IF crystals.

Crystal Orientation in Spherulites. The X-ray diffraction and polarized FTIR studies of spherulites of the PEO–pnp complex show that the two breaks observed in the log G versus T_c curves correspond to changes in the crystallographic growth face. In fact, the α_I and α_{III} spherulites which were obtained at low and high T_c

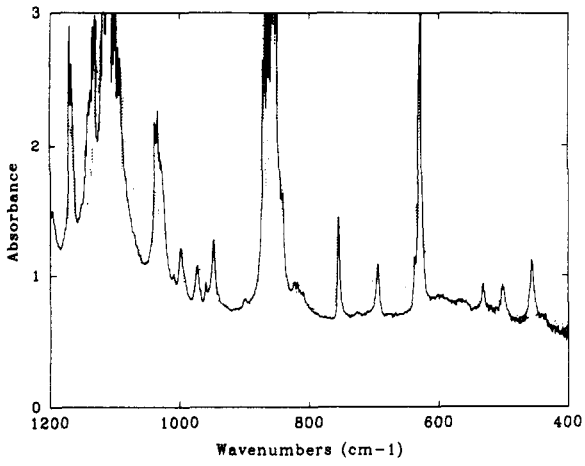

Figure 10. Polarized IR spectra of PEO(M_w=35 000)-pnp spherulites crystallized at 70 °C. The solid or broken lines correspond to an electric vector parallel or perpendicular to the radius of the spherulite, respectively.

Table I
Dichroism Observed for the pnp Vibrations

mode	wavenumber (cm^{-1})	M_w = 35 000, T_c = 50 °C	M_w = 35 000, T_c = 61 °C	M_w = 35 000, T_c = 67 °C	M_w = 6000, T_c = 50 °C	M_w = 6000, T_c = 60 °C
a1						
6a	630	∥	⊥	∥	∥	⊥
19a	1500		⊥		∥	⊥
8a	1612	∥	⊥	∥	∥	⊥
b2						
16b	501	⊥	1	⊥	⊥	1
4	694	⊥	1	⊥	⊥	1
11	755	⊥				
17b	851	⊥	1		⊥	
b1						
8b	1589		1		∥	
20b	3084	⊥	∥	⊥	⊥	∥
r_{NO_2}	531	⊥	∥	⊥	⊥	1
s_{NO_2}	863	∥	⊥	∥	∥	⊥
ν_{asNO_2}	1512		∥		⊥	

Table II
Dichroism Observed for the PEO Vibrations

mode	wavenumber (cm^{-1})	M_w = 35 000, T_c = 50 °C	M_w = 35 000, T_c = 61 °C	M_w = 35 000, T_c = 67 °C	M_w = 6000, T_c = 50 °C	M_w = 6000, T_c = 60 °C
b_u	455	∥	⊥	∥	∥	⊥
r_{CH_2}	872	⊥	∥		⊥	∥
a_u	948	⊥	⊥	1	⊥	⊥
b_u	1032	∥	⊥	∥	∥	⊥
b_u	1135	∥	⊥	∥	∥	⊥

crystallize with a (100) growth face, while the α_{II} spherulites which were observed in the intermediate range of T_c crystallize with a (010) growth face. We note here that similar results have been obtained for pure PEO[11,17,18] and for the PEO–*p*-dihalogenobenzene intercalates.[27] The orientation of the PEO macromolecules may be questioned on the basis of our observations. In the case of the (100) growth face, we can consider that the macromolecules fold more or less along the (100) plane as proposed in the case of the pure polymer. But, in the case of the (010) growth face, we have two different interpretations, first, the macromolecules may be folded along the (010) plane, in which case, the fold must be very large to include the pnp molecules between the PEO stems. This might account for the first break and also imply a reduction of crystallinity. This last point requires further investigations and is still in active progress. Second, we may consider that the macromolecules fold along the (100) plane. But, in this case, the plane of the PEO chains must be parallel to the growth direction, which is contrary to the usual description of polymer crystallization. However, Sadler considered this possibility in his model of rough surface growth.[28]

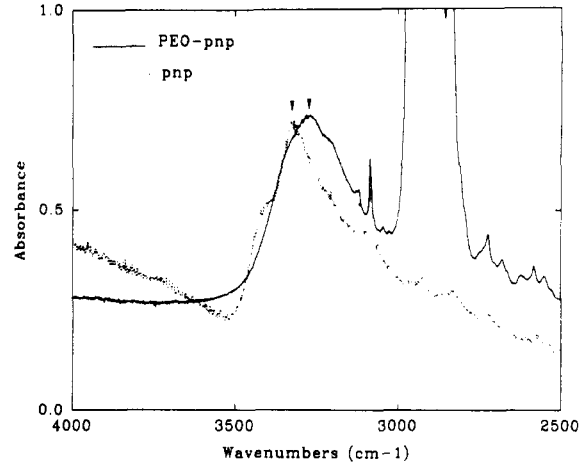

Figure 11. IR spectra of the OH stretching vibration of pure pnp and the PEO–pnp complex.

Finally, it is usual to linearize the log G versus $1/T\Delta T$ curves with a Williams–Landel–Ferry equation (β factor) which takes into account the increase in viscosity of the melt observed at low T_c.[8] But, despite the fact that the different regions in our curves correspond to the same melt, two different sets of parameters for the WLF equations are required to linearize these three regions which are related to the crystallization of (100) and (010) faces (Figures 2 and 3). In order, to use the retardation factor, it is necessary to take into account not only the thermal dependence of the chain moibility in the melt but also the mode of crystallization. In fact, by considering a simplified model for the growth of a molecular complex, the (100) growth face proceeds by successive deposition of layers of PEO and pnp molecules. On the contrary, the (010) face proceeds by simultaneous deposition of PEO and pnp molecules. Conceptually and as usually accepted, the WLF parameters U^* and T_∞ are intrinsic properties of the melt which may be estimated by measurement of the viscosity and/or by determination of the mobility of molecules by NMR. Thus, modifying the values of U^* and T_∞ to linearize the growth rate curves appears to be a dubious procedure. In the present case, and very likely in any case, this appears to be a mathematical game without any exact physical justification.

Conclusions

We have measured linear growth rates of spherulites of the PEO–pnp complex (M_w = 6000 and 35 000) from T_c = 25 to 70 °C. The log G versus T_c curves are surprisingly similar and show two breaks at 58 and 65 °C, the same transition temperatures for both molecular weights. From X-ray diffraction and polarized FTIR studies on PEO–pnp spherulites crystallized at different T_c, we have found that, for crystallization temperature below 58 °C and above 65 °C, the growth face corresponds to a (100) crystallographic face and that, in between these temperatures, the leading facet corresponds to a (010) face. Thus, we have demonstrated that the observed breaks in the curve giving the thermal dependence of the linear growth rate are not necessarily signatures of regime transitions, but it may also reveal morphological changes in the spherulites.

Acknowledgment. The authors are indebted to Dr. J. J. Janimak for fruitful discussions about the interpretation of kinetic data and about the Hoffman–Lauritzen theory of crystallization. This work was supported by the "Ministère de la Région Wallonne", research program FIRST, and by the "Fonds National de la Recherche Scientifique" (Belgium).

References and Notes

(1) Iwamoto, R.; Saito, Y.; Ishihara, H.; Tadokoro, H. *J. Polym. Sci. Polym. Phys. Ed.* **1969**, *6*, 1509.
(2) Chatani, Y.; Okamura, S. *Polymer* **1987**, *28*, 1815.
(3) Point, J. J.; Coutelier, C. *J. Polym. Sci., Polym. Phys. Ed.* **1985**, *23*, 231.
(4) Miyasnikova, R. M.; Titova, E. V.; Obolonkova, E. S. *Polymer* **1980**, *21*, 403.
(5) Delaite, E.; Point, J. J.; Damman, P.; Dosière, M. *Macromolecules* **1992**, *25*, 4768.
(6) Point, J. J.; Damman, P. *Macromolecules* **1992**, *25*, 1184.
(7) Damman, P.; Point, J. J., submitted to *Macromolecules*.
(8) Hoffmann, J. D.; Davis, G. T.; Lauritzen, J. I. *Treatise on solid state chemistry*; Hannay, N. B., Ed.; Plenum Press: New York, 1976; Vol. 3.
(9) Hoffmann, J. D. *Macromolecules* **1983**, *24*, 3.
(10) Allen, R. C.; Mandelkern, L. *Polym. Bull.* **1987**, *17*, 473.
(11) Point, J. J.; Damman, P.; Janimak, J. J., submitted to *Polymer*.
(12) Point, J. J.; Janimak, J. J., submitted to *J. Cryst. Growth*.
(13) Arlie, J. P.; Spegt, P.; Skoulios, A. *Makromol. Chem.* **1966**, *99*, 160. Arlie, J. P.; Spegt, P.; Skoulios, A. *Makromol. Chem.* **1967**, *104*, 212.
(14) Buckley, C. P.; Kovacs, A. J. *Kolloid Z. Z. Polym.* **1976**, *254*, 695.
(15) Cheng, S. Z. D.; Chen, J.; Barley, J. S.; Zhang, A.; Hanenschuss, A.; Zschak, P. R. *Macromolecules* **1992**, *25*, 1453.
(16) Kovacs, A. J.; Gonthier, A. *Kollid Z. Z. Polym.* **1972**, *250*, 530.
(17) Hirai, N.; Yashimata, Y.; Yokoyama, F. *Kobunshi Kagaku* **1964**, *21*, 724.
(18) Balta-Calleja, F. J.; Hay, I. L.; Keller, A. *Kolloid Z. Z. Polym.* **1966**, *209*, 128.
(19) Keith, H. D.; Padden, F. J. *J. Appl. Phys.* **1963**, *34*, 2409.
(20) Geil, P. H. *Polymer single crystals*; Interscience: New York, 1963.
(21) Damman, P. Thèse de doctorat, Université de Mons Hainaut, Mons, Belgium, 1992.
(22) Shimada, T.; Okui, N.; Kawai, T. *Makromol. Chem.* **1980**, *181*, 2643.
(23) Thierry, A.; Skoulios, A. *Eur. Polym. J.* **1977**, *13*, 169.
(24) Fraser, M. J.; Marshall, A.; Booth, C. *Polymer* **1977**, *18*, 93.
(25) Cheng, S. Z. D.; Chen, J.; Zhang, A.; Heberer, D. J. *J. Polym. Sci., Polym. Phys.* **1991**, *29*, 299.
(26) Ungar, G.; Keller, A. *Polymer* **1986**, *27*, 1835.
(27) Point, J. J.; Damman, P. *Macromolecules* **1991**, *24*, 2019.
(28) Sadler, D. M. *Nature* **1987**, *326*, 174.